Midinfrared absorption and photocurrent spectroscopy of InAs/GaAs self-assembled quantum dots

S. Sauvage, P. Boucaud,[a] and T. Brunhes
Institut d'Electronique Fondamentale, UMR CNRS 8622, Bâtiment 220, Université Paris-Sud, 91405 Orsay, France

V. Immer and E. Finkman
Department of Electrical Engineering and Solid State Institute, Technion Haifa 32000, Israel

J.-M. Gérard
Laboratoire CDP/URA 250, 196 Av. H. Ravéra, 92225 Bagneux, France

(Received 1 December 2000; accepted for publication 19 February 2001)

We report on a comparison between the midinfrared absorption and the photocurrent response of *n*-doped InAs/GaAs self-assembled quantum dots. The absorption, resonant at 160 meV, is polarized along the *z* growth axis of the dots. The photocurrent is dominated by a *z*-polarized resonance around 220 meV (5.6 μm wavelength). A weaker component of the photocurrent is observed for an in-plane polarized excitation. The photoresponse can be measured for a 0 V applied bias. The photoresponsivity is investigated as a function of the applied bias. The responsivity and the dark current exhibit an asymmetric profile versus the external bias. This asymmetry is correlated to the structural asymmetry of the quantum dot layers. © *2001 American Institute of Physics.*
[DOI: 10.1063/1.1365411]

Midinfrared photocurrent spectroscopy of In(Ga)As/GaAs self-assembled quantum dots has attracted a considerable interest in recent years.[1–5] The main objective of these studies was to investigate the properties of midinfrared quantum dot photodetectors, based on an operating principle similar to that of quantum well intersubband photodetectors.[6] These photodetectors could be of interest for long wavelength infrared imaging applications. The photoconductivity measurements reported in the literature were performed with different type of self-assembled quantum dots (InGaAs/GaAs, InAs/GaAs) under different experimental configurations, including normal incidence geometry,[1–3] wedge coupling geometry,[4,5] and lateral photocurrent measurements.[7] Whereas a detailed analysis of the photodetector performances was reported in some cases, a comparison between the midinfrared absorption associated with the intersublevel transition of the dots, its polarization, and the photocurrent is of significant interest.

In this letter, we report on a direct comparison between the midinfrared absorption of the self-assembled quantum dots and the photocurrent spectroscopy. All measurements are performed on the same sample. The InAs/GaAs self-assembled quantum dots were grown by molecular beam epitaxy on a semi-insulating GaAs substrate. The quantum dots have a lens shape geometry with a typical height of 2.5 nm and a lateral size of 20 nm. The investigated structure consists of a 594 nm thick n^+ (10^{18} cm^{-3}) GaAs bottom layer, a 200 nm thick nonintentionally doped GaAs layer, 20 periods of InAs quantum dots separated by 6.6 nm thick GaAs barriers, a 200 nm thick nonintentionally doped GaAs layer and a 594 nm thick n^+ GaAs top layer. The dot density is around 4×10^{10} cm^{-2}. The barriers between the self-assembled dots are uniformly *n*-doped with Si corresponding to a sheet carrier density of 7×10^{10} cm^{-2}. We emphasize that despite the small distance separating the quantum dot layers, there is no significant electronic coupling between the quantum dot ground states. 200×200 μm^2 mesa devices were fabricated using standard photolithography techniques. Ti/Au was evaporated to contact the layers. The processed samples were polished with a 45° wedge to test the polarization dependence of the photocurrent.

Figure 1 shows the midinfrared absorption of the *n*-doped sample measured at room temperature. The inset shows the low-temperature photoluminescence of the sample. The photoluminescence around 1.5 eV corresponds to the radiative recombination in the GaAs doped and undoped layers. The photoluminescence of the quantum dots is maximum at 1.18 eV with a full-width-at-half maximum of 80 meV. A smaller resonance below 1.1 eV is attributed to a

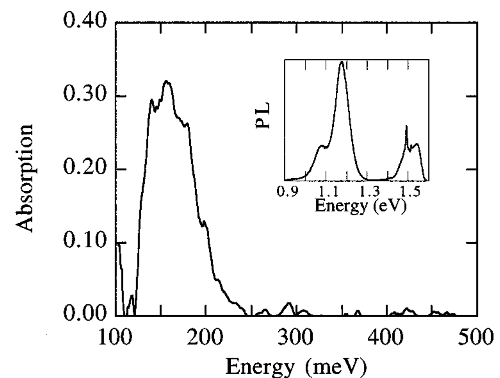

FIG. 1. Midinfrared absorption of the *n*-doped quantum dot sample measured in the multipass waveguide geometry. The absorption is deduced from the ratio of the transmission in *p* and *s* polarization. This transmission ratio is normalized by the transmission ratio measured with a bulk GaAs substrate. The inset shows the low-temperature (5 K) photoluminescence.

[a]Electronic mail: phill@ief.u-psud.fr

 © 2001 American Institute of Physics
Downloaded 11 Apr 2001 to 194.199.156.169. Redistribution subject to AIP copyright, see http://ojps.aip.org/aplo/aplcr.jsp

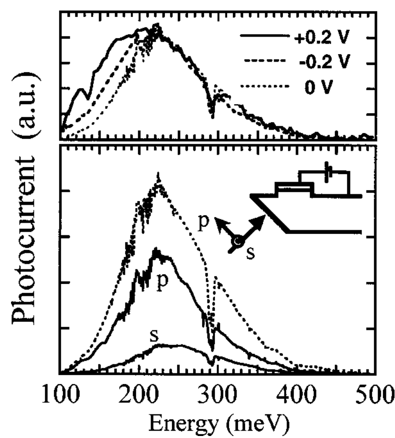

FIG. 2. Low-temperature (20 K) photocurrent measured for a *p*-polarized, a *s*-polarized and an unpolarized infrared excitation. The wedge coupling geometry is shown. The applied bias is 0 V. The dip at 290 meV is attributed to a CO_2 absorption line. Water absorption is also observed around 200 meV. The upper part shows the dependence of the photocurrent for an unpolarized excitation as a function of the applied bias: +0.2 V (full line), 0 V (dotted line), and −0.2 V (dashed line).

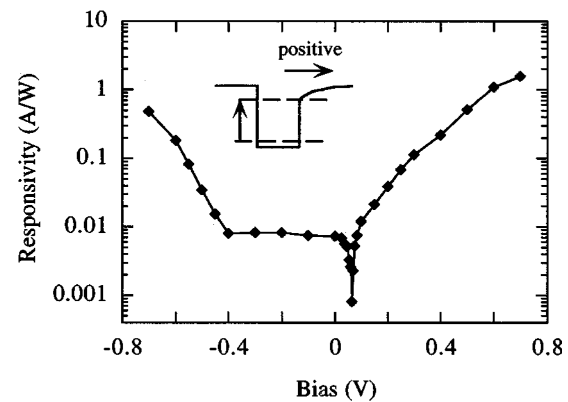

FIG. 3. Low-temperature (20 K) photoresponsivity as a function of the applied bias. The inset schematically illustrates the potential profile of the dots and the bias convention: at negative bias, the carriers escape towards the wetting layer side (left-hand side) of the dots. The vertical arrow indicates the absorption from the ground state to the wetting layer states.

small number of quantum dot layers with a reduced confinement of around 2 monolayers along the *z* direction. The absorption was measured in a multipass waveguide geometry obtained by polishing facets with a 45° angle. The length of the sample was adjusted in order to provide 25 reflections through the quantum dot layers. The absorption is deduced from the ratio of the transmittance in *p* and *s* polarizations. Above 100 meV, the absorption is dominated by a strong resonance around 160 meV (8 μm wavelength) with an amplitude of about 30%. The full-width at half maximum of the absorption is ~60 meV. This absorption, which is polarized along the *z* growth axis of the dots, is attributed to transitions from the dot grounds states to the wetting layer continuum states,[8] in agreement with previously reported results on self-assembled quantum dots.[9] We emphasize that the absorption is clearly dominated by a *z*-polarized transition although most of the photoconductivity measurements reported in the literature were performed using a normal incidence geometry. The performances of the detectors are not expected to be optimized in this case. Assuming that all carriers are transferred into the dots at room temperature, the absorption cross section for one quantum dot plane is 2.3×10^{-14} cm^{-2}. This absorption cross section is of the same order of magnitude than the absorption cross section reported for quantum well intersubband photodetectors.[10] This cross section is larger than the one reported in Ref. 9. The difference is explained by a smaller broadening of the absorption in the present case along with a more efficient charge transfer into the dots. Recently, the measurement of the absorption amplitude of the *s*–*p* transition[11] has indeed shown that for the sample investigated in Ref. 9, only 2×10^{10} cm^{-2} instead of the assumed 8×10^{10} cm^{-2} carriers were transferred at room temperature into the dots. This nontotal transfer of the carriers into the dots led to an underestimation of the absorption cross section.

Figure 2 shows the photocurrent measured at 20 K, for *p*- and *s*- polarized midinfrared excitations. The dashed line corresponds to an unpolarized midinfrared excitation. The inset shows the wedge coupling geometry. In *p* polarization, the components of the electric field are along the *z* direction and in the layer plane. The applied bias was 0 V. In agreement with the absorption measurements, the photocurrent is found significantly larger in *p* polarization than in *s* polarization. The photocurrent measured in *s* polarization indicates that the device can be operated in a normal incidence geometry. A similar photocurrent spectral dependence was indeed observed for an in-plane incident geometry (not shown). The photocurrent exhibits an asymmetric line shape with a maximum around 225 meV, indicating a significant blueshift as compared to the absorption (160 meV). The broadening of the photocurrent is ~120 meV. The blueshift of the resonance is attributed to the different nature of the involved processes. The oscillator strength of the absorption is maximum for transitions from the ground state to the two-dimensional wetting layer states. The photocurrent results from a sequential mechanism, i.e., the photoexcitation of the carriers followed by their escape out of the dots. The influence of the escape probability explains that the photoresponsivity at low applied bias is likely to be maximum at an energy associated with the transitions from the ground states to the continuum states. In a previous application, we did report by photoinduced absorption measurements on a 30 meV energy difference between intraband transitions to the wetting layer states or to the GaAs continuum.[12] The 65 meV blueshift presently observed is larger than this shift. This difference indicates the importance of the dependence of the photoconductive gain as a function of the energy.[13] The stacking of the multiple layers should also be considered in order to describe the continuum states.[14]

Figure 3 shows the peak photoresponsivity measured at 20 K in wedge illumination as a function of the applied bias. The response is given up to 0.6 V. The applied bias which corresponds in this case to a ~10 kV/cm electric field is limited by the saturation of the current amplifier by the dark current.[15] The calibrated response was measured with a 1000 K blackbody source. Two distinct features are highlighted in Fig. 3. The minimum of responsivity is not obtained at 0 V applied bias but for a positive applied bias (0.065 V). This feature results from an asymmetry in the device introduced by the doping and the existence of a built-in electric field.[4] It is worth noting that the photoresponse can be easily mea-

Downloaded 11 Apr 2001 to 194.199.156.169. Redistribution subject to AIP copyright, see http://ojps.aip.org/aplo/aplcr.jsp

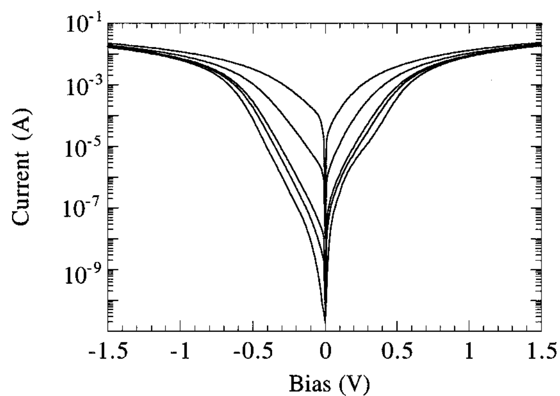

FIG. 4. Current–voltage characteristic of the device as a function of the temperature. From bottom to top (35–45–50–67–90 K).

sured at 0 V with a peak responsivity reaching 8 mA/W. The second feature is related to the asymmetry of the photoresponse. The photoresponse first saturates at negative applied bias then increases rapidly at higher negative applied biases. This rapid increase is a signature of the enhancement of the field-assisted tunneling. As the negative applied bias increases, a broadening of the photocurrent is observed in the low energy spectral range. For positive biases, the photocurrent increases continuously at positive applied biases. A significant redshift of the peak responsivity is observed in this case; the photocurrent is resonant at 200 meV for a 0.2 V applied bias. The broadening and the redshift of the photoresponse are very similar to those reported for multiquantum well intersubband photodetectors with graded barriers.[16] It indicates that the confinement potential profile is likely to exhibit a similar type of grading along the z growth axis. This grading would result from the intermixing between In and Ga, the strain relaxation, and most importantly from the In segregation. Scanning tunneling spectroscopy on the InAs self-assembled dots has shown that the transition from the top of the dot to the GaAs layer is gradual and associated with InGaAs alloying.[17] The corresponding potential profile is schematically illustrated in the inset of Fig. 3. The effective barrier height is *a priori* lower on the side opposite to the wetting layer. As the positive applied bias increases, the resonance of the photocurrent is redshifted towards the low-energy barrier height. For negative applied biases, the peak resonance of the photocurrent is not expected to shift. The photocurrent should however be increased in the low-energy side because of the enhancement of the absorption followed by field-assisted tunneling. We note that the potential profile depicted in Fig. 3 implies, as experimentally observed, a blueshift of the photocurrent resonance as compared to the absorption.

The asymmetry in the responsivity is also observed in the dark current, as shown in Fig. 4. The current–voltage measurements were taken with a cooled radiation shield around the sample. It is well known that in quantum well photodetectors, the asymmetry of the interfaces induces an asymmetry in the dark current versus the applied bias.[6] The quantum dots grown on top of a wetting layer with a lens-shape geometry have an intrinsic asymmetric potential profile. The asymmetry can be enhanced by segregation and intermixing as shown in the inset of Fig. 3. Therefore, one also expects the dark current to reflect the structural asymmetry of the quantum dots and their interfaces. This feature is illustrated in Fig. 4. At low temperature (35 K), the dark current which is governed by a thermally-assisted tunneling mechanism[18] is larger for a positive applied bias as compared to the corresponding negative applied bias. At negative applied bias, the escape of the carriers from the dot occurs from the side of the dots close from the wetting layer. The potential profile shown in the inset of Fig. 3 qualitatively explains the dark current measurements. The effective barrier height is lower for positive applied bias as compared to the negative applied bias. The thermally assisted tunneling will therefore be larger for positive bias. We note that at higher temperatures (90 K), the dark current is dominated by the thermionic emission and does not exhibit such asymmetry.

In conclusion, we have investigated the midinfrared absorption and the photocurrent spectroscopy of n-doped InAs/GaAs self-assembled quantum dots. The absorption in the midinfrared spectral range is dominated by a z-polarized intraband transition from the ground state to the wetting layer states. The photocurrent is also maximum for a z-polarized excitation. The photocurrent is blueshifted as compared to the absorption. The asymmetry of the photoresponsivity and of the dark current suggests an asymmetric confinement potential barrier. The present structure was not designed to minimize the dark current. Further work is in progress to evaluate the detector performances in optimized structures.

[1] K. W. Berryman, S. A. Lyon, and M. Segev, Appl. Phys. Lett. **70**, 1861 (1997).
[2] D. Pan, E. Towe, and S. Kennerly, Appl. Phys. Lett. **73**, 1937 (1998).
[3] S. Kim, H. Mohseni, M. Erdtmann, E. Michel, C. Jelen, and M. Razeghi, Appl. Phys. Lett. **73**, 963 (1998).
[4] S. Maimon, E. Finkman, G. Bahir, S. E. Schacham, J. M. Garcia, and P. M. Petroff, Appl. Phys. Lett. **73**, 2003 (1998).
[5] L. Chu, A. Zrenner, G. Böhm, and G. Abstreiter, Appl. Phys. Lett. **75**, 3599 (1999).
[6] B. F. Levine, J. Appl. Phys. **74**, R1 (1993).
[7] L. Chu, A. Zrenner, G. Böhm, and G. Abstreiter, Appl. Phys. Lett. **76**, 1944 (2000).
[8] The self-assembled quantum dots are grown on top of an InAs wetting layer. Outside from the dots, the wetting layer is equivalent to a thin quantum well. The associated confined states correspond to a quantum well like two-dimensional continuum. Few states are confined in these lens-shaped quantum dots. The first excited state is around 60 meV above the ground state. The next confined states are very close to the two-dimensional wetting layer states. For these states, the wave function is significantly delocalized in the layer plane.
[9] S. Sauvage, P. Boucaud, F. H. Julien, J.-M. Gérard, and V. Thierry-Mieg, Appl. Phys. Lett. **71**, 2785 (1997).
[10] J. Y. Duboz, E. Costard, J. Nagle, J. M. Berset, J. M. Ortega, and J. M. Gérard, J. Appl. Phys. **78**, 1224 (1995).
[11] S. Sauvage, P. Boucaud, T. Brunhes, F. Glotin, R. Prazeres, J.-M. Ortéga, and J.-M. Gérard, Phys. Rev. B **63**, 113312 (2001).
[12] S. Sauvage, P. Boucaud, J.-M. Gérard, and V. Thierry-Mieg, Phys. Rev. B **58**, 10562 (1998).
[13] H. C. Liu, Appl. Phys. Lett. **60**, 1507 (1992).
[14] A. Fraenkel, A. Brandel, G. Bahir, E. Finkman, G. Livescu, and M. T. Asom, Appl. Phys. Lett. **61**, 1341 (1992).
[15] The small thickness of the active region limits the applied bias.
[16] B. F. Levine, C. G. Bethea, V. O. Shen, and R. J. Malik, Appl. Phys. Lett. **57**, 383 (1990).
[17] B. Legrand, B. Grandidier, J. P. Nys, D. Stievenard, J. M. Gérard, and V. Thierry-Mieg, Appl. Phys. Lett. **73**, 96 (1998).
[18] P. Kolev, M. J. Deen, H. C. Liu, J. M. Li, M. Buchanan, and Z. R. Wasilewski, J. Appl. Phys. **87**, 2400 (2000).

Downloaded 11 Apr 2001 to 194.199.156.169. Redistribution subject to AIP copyright, see http://ojps.aip.org/aplo/aplcr.jsp